催 化 学 报

2011　　Chinese Journal of Catalysis　　Vol. 32 No. 4

文章编号: 0253-9837(2011)04-0572-10　　**国际版 DOI**: 10.1016/S1872-2067(10)60191-X　　**研究论文:** 572~581

低温等离子体处理对 NiO/Al_2O_3 吸附 NO_x 的促进作用

李秋荣[1,2,*], 武金宝[1], 郝吉明[2]

[1]燕山大学环境与化学工程学院, 河北秦皇岛 066004

[2]清华大学环境科学与工程系, 北京 100084

摘要: 采用共沉淀法制备了不同 NiO 负载量的 NiO/Al_2O_3 催化剂, 并用于 NO_x 储存还原技术去除 NO_x 反应中. 结果表明, 当 Ni/Al 摩尔比为 0.3 时, NiO/Al_2O_3 样品的 NO_x 吸附量最大; 随着 Ni 含量的增加, $NiAl_2O_4$ 晶相减少. 沉淀物在高温煅烧前利用低温等离子体处理后, 所得催化剂吸附 NO_x 的能力明显增强, 当 Ni/Al 摩尔比为 0.3 的催化剂, NO_x 吸附量由未处理时的 345 μmol/g 增至经处理后的 477 μmol/g. 研究发现, 经低温等离子体处理后, 催化剂上粒子更加分散, 比表面积增大. 另外, 利用原位红外光谱分析了催化剂吸附 NO_x 的机理. 结果表明, 吸附的 NO 首先在催化剂表面以桥式亚硝酸盐形式存在, 然后转变成不同形式的硝酸盐.

关键词: 氧化镍; 氧化铝; 氮氧化物; 低温等离子体; 吸附; 储存量; 稀燃发动机

中图分类号: O643　　**文献标识码:** A

收稿日期: 2010-11-05. 接受日期: 2011-01-07.

*通讯联系人. Tel: (0335) 8387744; Fax: (0335) 8061569; E-mail: qiurong@ysu.edu.cn

基金来源: 国家自然科学基金 (51078203); 国家高技术研究发展计划 (863 计划, 2010AA065002); 河北省教育厅科学研究项目 (2009481).

本文的英文电子版(国际版)由Elsevier出版社在ScienceDirect上出版(http://www.sciencedirect.com/science/journal/18722067).

NO_x Storage Capacity Enhancement on NiO/Al_2O_3 Pretreated with a Non-thermal Plasma

LI Qiurong[1,2,*], WU Jinbao[1], HAO Jiming[2]

[1]*College of Environmental and Chemical Engineering, Yanshan University, Qinhuangdao 066004, China*

[2]*Department of Environmental Science and Engineering, Tsinghua University, Beijing 100084, China*

Abstract: In the NO_x storage reduction (NSR) technology used to remove NO_x from lean burn engines, the NO_x storage material is crucial. For NiO/Al_2O_3 catalysts with different NiO loading prepared by coprecipitation, the maximum storage capacity for NO_x occurred at a Ni/Al molar ratio of 0.3 in the catalyst. The intensity of the $NiAl_2O_4$ diffraction peak decreased with increased nickel content. When the catalysts were pretreated by a non-thermal plasma (NTP) before calcination at high temperature, the adsorption capacities for NO_x increased, with an increase from 345 to 477 μmol/g on the NiO/Al_2O_3 catalyst with the Ni/Al molar ratio of 0.3. The metal dispersion was increased with the NTP treatment, which resulted in a high surface area. The NO_x storage mechanism was discussed on the basis of DRIFTS results, which indicated that NO was first adsorbed on the surface as bridged nitrites, and then the nitrites species was transformed into different kinds of NO_3^- adsorbed species.

Key words: nickel oxide; aluminum oxide; nitric oxides; non-thermal plasma; adsorption; storage capacity; lean burn engine

Received 5 November 2010. Accepted 7 January 2011.

**Corresponding author. Tel: +86-335-8387744; Fax: +86-335-8061569; E-mail: qiurong@ysu.edu.cn*

This work was supported by the National Natural Science Foundation of China (51078203), the National High Technology Research and Development Program of China (863 Program, 2010AA065002), and the Research Project of Department of Education of Hebei Province (2009481).

English edition available online at Elsevier ScienceDirect (http://www.sciencedirect.com/science/journal/18722067).

十多年来, 氮氧化物 (NO_x) 储存还原 (NSR) 技术　　一直应用于稀燃发动机的废气处理中. 在常规 NSR

催化剂(如$Pt/BaO/Al_2O_3$)中, 贵金属是催化剂的活性组分, 而碱土金属氧化物在NO_x储存方面起着重要作用[1~7]. 由于在200~500 ºC的较宽的温度范围内, NSR催化剂在低温下应具有较大的NO_x储存能力[8,9]. 考虑到贵金属催化剂的高成本, 人们一直尝试过渡金属氧化物(尤其是NiO), 因具有良好的催化性能而被用于许多反应过程[10~15], 另外, 低温等离子体(NTP)处理Ni基催化剂可极大改善其性能[16,17]. 然而, 有关于Ni基催化剂的NO_x吸附性能的研究尚未见报道. 本文采用共沉淀法制备NiO/Al_2O_3催化剂, 并在高温煅烧前用低温等离子体处理. 考察其低温储存NO_x的能力, 并探讨其储存NO_x的机理.

1 实验部分

1.1 催化剂的制备

采用共沉淀法制备NiO/Al_2O_3催化剂. 先将200 ml 0.6 mol/L的$Al(NO_3)_3$溶液和一定量聚乙二醇加入到500 ml三颈瓶中, 再加入沉淀剂$(NH_4)_2CO_3$, 在70 ºC搅拌6 h后, 分别按Ni/Al摩尔比为0.15, 0.3, 0.45, 0.6, 和1.0加入硝酸镍溶液[18]. 溶液pH值调为9, 所得溶胶于70 ºC老化, 过滤, 干燥后, 在330 ºC煅烧3 h, 然后升至550 ºC煅烧2.5 h, 所得催化剂分别记为NiO/Al_2O_3-0.15(C), NiO/Al_2O_3-0.3(C), NiO/Al_2O_3-0.45(C), NiO/Al_2O_3-0.6(C)和NiO/Al_2O_3-1.0(C).

低温等离子体的装置参见文献[19]. 将上述所得不同Ni/Al摩尔比的溶胶经330 ºC煅烧3 h后, 利用NTP处理(放电功率为80 W) 30 min后, 再在550 ºC煅烧2 h, 所得样品依次标记为NiO/Al_2O_3-0.15(P), NiO/Al_2O_3-0.3(P), NiO/Al_2O_3-0.45(P), NiO/Al_2O_3-0.6(P)和NiO/Al_2O_3-1.0(P).

1.2 催化剂的表征

样品比表面积测定在NOVA4000e型比表面积分析仪上进行. 实验前样品于300 ºC脱气2 h, 以N_2为吸附质于–196 ºC下进行.

样品X射线衍射(XRD)实验采用TTR-Ⅲ型粉末XRD仪, Cu靶光源, 管电压60 kV, 电流300 mA, 扫描范围10°~90°, 扫描速率为4°/min.

程序升温还原(H_2-TPR)测试在Micromeritics ChemiSorb 2720型自动装置上进行, 采用U形石英管反应器, 样品用量为50 mg. 样品于300 ºC通N_2预处理30 min, 冷却至室温. 切换为10% H_2-90% Ar混合气, 控制混为50 ml/min, 待记录仪基线平稳后, 以10 ºC/min升温至1000 ºC. TCD检测器检测耗H_2量.

采用JEOL 200CX型透射电镜(TEM)观察样品形貌和粒径.

催化剂样品用VG Scientific ESCALab220i-XL型光电子能谱(XPS)仪分析. 激发源为Mg K_α射线, 功率为300 W. 分析时基础真空为3×10^{-7} Pa. 电子结合能用无定形碳的C 1*s* (284.8 eV)校正. 测定C 1*s*, O 1*s*, Ni 2*p*和Al 2*p*的结合能. 实验所得数据用XPSPEAK软件处理(Gaussian/Lorantzia比为90/10).

催化剂表面反应物吸附态及中间物种通过漫反射原位池和高灵敏度液氮冷却MCT检测器的Nicolet Nexus 870-FTIR型傅里叶红外光谱仪分析. 扫描范围4000~400 cm^{-1}, 分辨率4 cm^{-1}, 扫描数100.

催化剂粉末试样直接置于原位池的样品台内并压实, 反应前于500 ºC经8% O_2-92% N_2混合气(400 ml/min)预处理30 min以除去表面杂质. 背景谱图是在指定温度下稳定20 min后采集, 样品谱图是在吸附开始后采集, 反应为0.05% NO, 8% O_2, N_2平衡, 总流量为100 ml/min. 吸附30 min后降温到50 ºC, 并用100 ml/min纯N_2吹扫1 h, 然后升温至各温度点进行脱附, 稳定20 min后采集图谱.

1.3 NO吸附-脱附

称取0.5 g催化剂放入内径为5 mm的U形石英管中, 在500 °C经8% O_2-92% N_2气流(400 ml/min)中预处理30 min后, 将反应器温度降到100 °C, 通入总流量为400 ml/min的0.05% NO + 8% O_2 + N_2(平衡气)吸附气体, 恒温吸附30 min. 采用NO-NO_2-NO_x分析仪在线测量反应前后NO_x浓度. 程序升温脱附(TPD)测试实验装置和催化剂装量同上, 且在上述实验之后进行. 将催化剂吸附0.05% NO + 8% O_2 + N_2(平衡气) 30 min后, 关闭NO和O_2后, 用N_2 (400 ml/min)吹扫1 h以除去催化剂表面物理吸附的NO_x, 然后以10 °C /min从常温升到500 °C, 使用NO-NO_2-NO_x分析仪检测脱附气体中NO、NO_2和NO_x浓度, 催化剂的NO_x储存量根据脱附峰面积计算.

2 结果与讨论

2.1 Ni负载量和NTP处理对催化剂NO_x储存能力的影响

表1为不同Ni含量的NiO/Al_2O_3催化剂的NO_x

表 1 各 NiO/Al_2O_3 催化剂在不同处理条件下的 NO_x 储存量和穿透时间

Table 1 NO_x storage capacity and break through time of different NiO/Al_2O_3 catalysts with different treatment conditions

Catalyst	Break through time (min)	NO_x storage capacity (μmol/g)
NiO/Al_2O_3-0.15(C)	5	283
NiO/Al_2O_3-0.15(P)	5.5	344
NiO/Al_2O_3-0.30(C)	5	345
NiO/Al_2O_3-0.30(P)	7	477
NiO/Al_2O_3-0.45(C)	5	330
NiO/Al_2O_3-0.45(P)	7	475
NiO/Al_2O_3-0.60(C)	5	316
NiO/Al_2O_3-0.60(P)	7	385
NiO/Al_2O_3-1.0(C)	4	268
NiO/Al_2O_3-1.0(P)	7	391

C—conventional method; P—plasma treatment method.

储存量和穿透时间. 由表可见, NiO/Al_2O_3-0.15(C), NiO/Al_2O_3-0.30(C), NiO/Al_2O_3-0.45(C) 和 NiO/Al_2O_3-0.60(C) 吸附穿透时间为 5 min, 而 NiO/Al_2O_3-1.0(C) 样品的为 4 min, 且当 Ni/Al 摩尔比为 0.3 时, 样品的 NO_x 储存能力达最大, 为 345 μmol/g. 催化剂经 NTP 处理后, 其吸附穿透时间明显延长. NiO/Al_2O_3-0.30(P), NiO/Al_2O_3-0.45(P), NiO/Al_2O_3-0.60(P) 和 NiO/Al_2O_3-1.0(P) 催化剂的吸附穿透时间为 7 min, 且 NiO/Al_2O_3-0.30(P) 样品的 NO_x 储存能力最大, 为 477 μmol/g, 比 NiO/Al_2O_3-0.30(C) 的提高了 38%. 吸附穿透后, 出口处 NO_x 浓度逐渐达到 0.07% 左右. 可见, 经 NTP 的催化剂需要较长时间达到吸附饱和. 由于 Ni/Al 摩尔比为 0.30 的 NiO/Al_2O_3 催化剂的 NO_x 储存能力最高, 下文有关催化剂表征主要采用该催化剂.

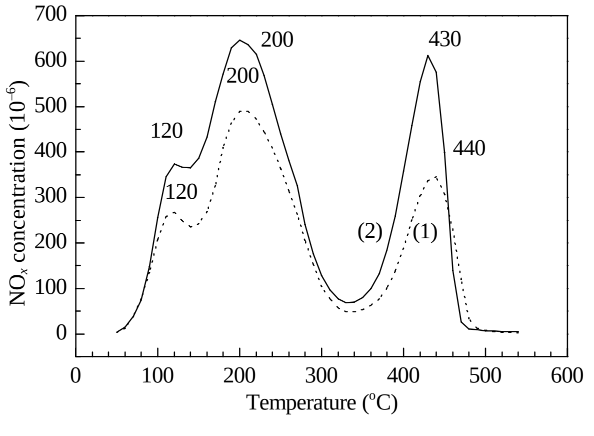

图 1 催化剂的 NO_x-TPD 谱

Fig. 1. NO_x-TPD profiles of NiO/Al_2O_3-0.30(C) (1) and NiO/Al_2O_3-0.30(P) (2) catalysts.

2.2 NTP 处理对催化剂 NO_x 脱附的影响

由表 1 可见, 经 NTP 处理后, 催化剂的 NO_x 储存能力显著增加. 图 1 为 NiO/Al_2O_3-0.30(C) 和 NiO/Al_2O_3-0.30(P) 的 NO_x-TPD 谱. 可以看出, 这两个催化剂分别在 120, 200 和 430 °C 附近出现三个脱附峰. 但经 NTP 处理催化剂的 NO_x 脱附量在低温和高温区明显增加. 120 °C 处的脱附峰应与偏铝酸镍有关, 随着镍含量的增加, 偏铝酸镍的峰减弱, 偏铝酸镍可能是 NO_x 储存能力的一个重要因素[18].

2.3 催化剂的表征

2.3.1 比表面积

表 2 为各催化剂的比表面积. 可以看出, 随着 Ni 负载量的增加, Ni 物种在载体表面发生聚集和堆积, 载体的一些孔道被堵塞, 导致 NiO 分散性变差, 因而催化剂的比表面积下降. 值得注意的是经 NTP 处理催化剂的比表面积明显增加, 这主要是由于 NTP 处理可以改善催化剂粒子的分散性.

表 2 经和未经 NTP 处理 NiO/Al_2O_3 催化剂的比表面积

Table 2 Specific surface area of NiO/Al_2O_3 catalysts with and without the NTP treatment

Catalyst	$A_{BET}/(m^2/g)$
NiO/Al_2O_3-0.15(C)	201.6
NiO/Al_2O_3-0.15(P)	225.9
NiO/Al_2O_3-0.30(C)	193.3
NiO/Al_2O_3-0.30(P)	213.7
NiO/Al_2O_3-0.45(C)	189.2
NiO/Al_2O_3-0.45(P)	206.3
NiO/Al_2O_3-0.60(C)	175.6
NiO/Al_2O_3-0.60(P)	190.2
NiO/Al_2O_3-1.0(C)	146.8
NiO/Al_2O_3-1.0(P)	169.2

2.3.2 XRD 结果

图 2 为不同 NiO/Al_2O_3 催化剂的 XRD 谱. 可以看出, Ni/Al 摩尔比为 0.15 和 0.30 时, NiO/Al_2O_3 样品于 19°, 31°, 37°, 45° 和 65° 处出现 $NiAl_2O_4$ 衍射峰, 且经 NTP 处理后样品的稍弱, 这是由于 NTP 处理使得 $NiAl_2O_4$ 晶粒变小所致[20], 但 NiO/Al_2O_3-0.30(P) 在 19° 的 $NiAl_2O_4$ 衍射峰则比 NiO/Al_2O_3-0.30(C) 的强.

经 NTP 处理后, Ni/Al 摩尔比为 0.60 和 1.0 的样品中 NiO 衍射峰强度增加, 且随着 Ni 含量增加, NiO 衍射峰增强. 这说明所得样品均具有良好的晶体结构. 另外, Ni/Al 摩尔比为 0.60 的 NiO/Al_2O_3 样品的 $NiAl_2O_4$ 峰形比摩尔比为 0.30 的弥散, 而当摩尔比为

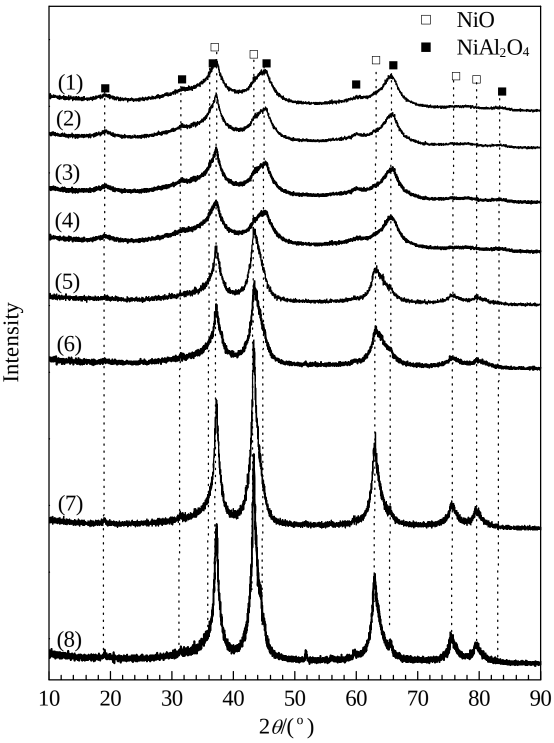

图 2　经和未经 NTP 处理 NiO/Al_2O_3 催化剂的 XRD 谱

Fig. 2. XRD patterns of NiO/Al_2O_3 catalysts with and without the NTP treatment. (1) NiO/Al_2O_3- 0.15(C); (2) NiO/Al_2O_3-0.15(P); (3) NiO/Al_2O_3-0.30(C); (4) NiO/ Al_2O_3-0.30(P); (5) NiO/Al_2O_3-0.60(C); (6 NiO/Al_2O_3-0.60(P); (7) NiO/Al_2O_3-1.0(C); (8) NiO/Al_2O_3-1.0(P).

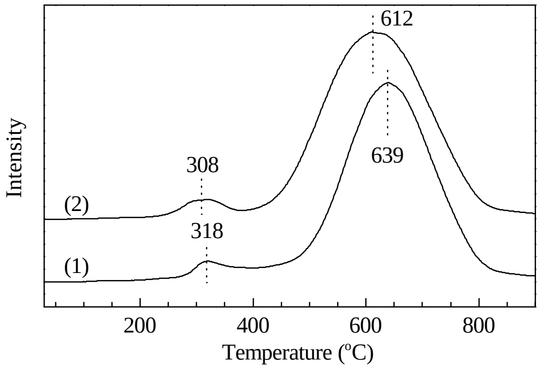

图 3　不同方法制备的 NiO/Al_2O_3 催化剂的 H_2-TPR 谱

Fig. 3. H_2-TPR profiles of NiO/Al_2O_3 catalysts prepared by the different methods. (1) NiO/Al_2O_3-0.30(C); (2) NiO/Al_2O_3-0.30(P).

1.0时基本消失. 结合样品的NO_x吸附量可知, Ni/Al摩尔比为 0.3 样品的吸附性能最好, 故可推测$NiAl_2O_4$可能是影响样品NO_x吸附性能的一个重要因素[18].

2.3.3　H_2-TPR 结果

图 3 为 NiO/Al_2O_3-0.30(C) 和 NiO/Al_2O_3-0.30(P) 样品的 H_2-TPR 谱. 可以看出, 催化剂出现 2 个耗 H_2 峰: NiO/Al_2O_3-0.30(C) 的分别位于 318 和 639 ºC, NiO/Al_2O_3-0.3(P) 的分别位于 308 和 612 ºC. 低温还原峰应归属于 Ni_2O_3→NiO 的还原, 高温还原峰则对应于 NiO→Ni. 可以看出, 经 NTP 处理后, 催化剂还原温度降低, 峰形变宽, 说明催化剂经 NTP 处理后更易于被还原, 更有利于 NO 的氧化.

2.3.4　TEM 结果

图 4 为 NiO/Al_2O_3-0.30(C) 和 NiO/Al_2O_3-0.30(P) 样品的 TEM 照片. 由图可见, NiO/Al_2O_3-0.30(C) 样品上的粒子分散不是非常均匀, NiO 团聚现象比较严重. 与 NiO/Al_2O_3-0.30(C) 相比, NiO/Al_2O_3-0.30(P) 的团聚现象则不是太明显, 粒子分布比较均匀. 利用等离子体物理和凝聚态物理研究低温等离子体处理催化剂的特性[21], 等离子体处理后催化剂的活性显著提高.

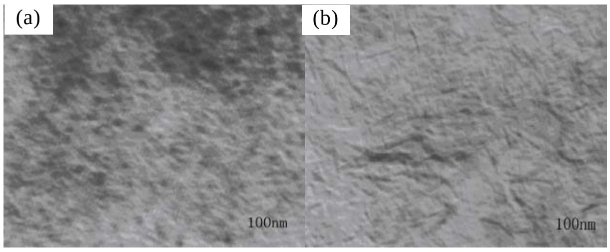

图 4　NiO/Al_2O_3-0.30(C) 和 NiO/Al_2O_3-0.30(P) 样品的 TEM 照片

Fig. 4. TEM images of NiO/Al_2O_3-0.30(C) (a) and NiO/Al_2O_3-0.30(P) (b) samples.

2.3.5　XPS 结果

不同方法制备的催化剂的 Ni $2p_{3/2}$ 结合能见图 5. 由图可见, NiO/Al_2O_3-0.30(C) 的 Ni $2p_{3/2}$ 主峰在 853.8 eV 处, 卫星峰在 859.9 eV, 自旋轨道耦合能间隙

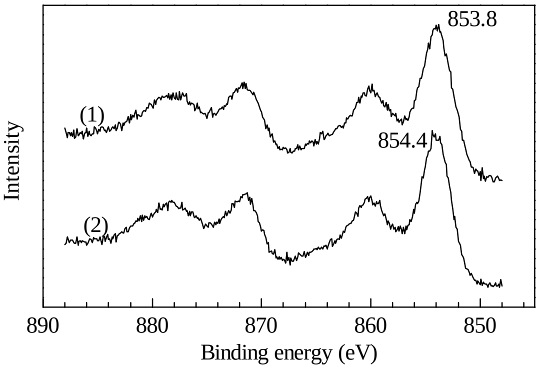

图 5　不同方法制备的 NiO/Al_2O_3 催化剂的 Ni $2p$ XPS 谱

Fig. 5. Ni $2p$ XPS spectra of NiO/Al_2O_3 catalysts prepared by the different methods. (1) NiO/Al_2O_3-0.30(C); (2) NiO/Al_2O_3-0.30(P).

表 3　NiO/Al_2O_3-0.30(C) 和 NiO/Al_2O_3-0.30(P) 催化剂表面元素的相对含量

Table 3　Relative amounts of the elements on NiO/Al_2O_3-0.30(C) and NiO/Al_2O_3-0.30(P) surface

Catalyst	Relative amounts (%)		
	O	Al	Ni
NiO/Al_2O_3-0.30(C)	69.59	22.45	7.96
NiO/Al_2O_3-0.30(P)	70.11	21.61	8.28

为 17.8 eV, 而 NiO/Al_2O_3-0.30(P) 样品的以上各峰分别出现在 854.4, 860 和 16.9 eV. NiO 和 $NiAl_2O_4$ 的 Ni $2p_{3/2}$ 结合能分别为 854.5 和 856 eV. 由上可见, NiO/Al_2O_3-0.30(P) 的 Ni $2p_{3/2}$ 结合能比 NiO/Al_2O_3-0.30(C) 的稍高, 这是由于它们表面元素含量差异所致[22]. 表 3 为这 2 个样品表面元素的相对含量. 可以看出, 经 NTP 处理后, 催化剂表面 O 和 Ni 的相对含量有所增加, 且其中偏铝酸镍的含量也略高, 所以 NiO/Al_2O_3-0.30(P) 的 Ni $2p_{3/2}$ 结合能比 NiO/Al_2O_3-0.30(C) 的高, 这与 NO_x-TPD 的结果一致.

2.4 FT-IR 结果

2.4.1 NO_x 吸附

图 6 为 NiO/Al_2O_3-0.30(C) 和 NiO/Al_2O_3-0.30(P) 催化剂在 100 ºC 吸附 NO 随时间变化的 DRIFT 谱. 可以看出, 催化剂表面吸附物种的吸收峰集中在 1000~1800 cm^{-1}, 其中 1040 cm^{-1} 可归属于 *cis*-$(N_2O_2)^{2-}$ 吸附物种, 1205 cm^{-1} 附近为桥式亚硝酸盐, 1260, 1400 和 1560 cm^{-1} 为不同形式的硝酸盐物种, 1620 cm^{-1} 可归属为气态 NO_2 的物理吸附[23,24].

对于 NiO/Al_2O_3-0.30(C) 样品, 吸附刚开始时, 在催化剂表面主要有桥式亚硝酸盐 (1215 cm^{-1}) 和弱 NO_2 吸附物种 (1624 cm^{-1})[25], 至 3 min 时, NO_2 的吸收峰比较明显, 并出现桥式硝酸盐 (1560 cm^{-1}) 物种. 吸附 5 min 时, 硝酸盐物种吸收峰明显增强. 至 7 min 时, 吸附物种转变为桥式亚硝酸盐 (1263 cm^{-1}), 单齿硝酸盐 (1296 cm^{-1}), 桥式硝酸盐和 NO_2 吸附物种. 至 10 min 时, *cis*-$(N_2O_2)^{2-}$ (1040 cm^{-1}) 吸附物种以及桥式亚硝酸盐, 单齿硝酸盐, 桥式硝酸盐和 NO_2 吸附物种吸收峰增强. 继续吸附至 30 min 时, 各吸附峰变化不大[26~29]. 对于 NiO/Al_2O_3-0.30(P) 样品, 吸附刚开始时, 催化剂表面主要以桥式亚硝酸盐 (1199~1223 cm^{-1}) 为主, 吸附 10 min 后, 吸附物种主要是桥式亚硝酸盐 (1269 cm^{-1}), 单齿硝酸盐 (1299 cm^{-1}), 桥式硝酸盐 (1542 cm^{-1}) 和少量气态 NO_2 物理吸附, 没有出现 *cis*-$(N_2O_2)^{2-}$ 的吸附物种. 另外, NiO/Al_2O_3-0.30(P) 样品的各吸收峰比 NiO/Al_2O_3-0.30(C) 的较宽.

2.4.2 NO_x 的脱附

NO_x 在 0.3 NiO/Al_2O_3(C) 和 0.3 NiO/Al_2O_3(P) 催化剂表面吸附 30 min 后, 停止 NO + O_2 进气, 改以相同气量 N_2 吹扫, 然后程序升温并采集 DRIFTS 谱, 结果见图 7. 对于 NiO/Al_2O_3-0.30(C) 样品, 200 ºC 时仍存在 NO_2 的物理吸收峰, 1294 和 1251 cm^{-1} 处的吸收带逐渐减弱, 并在 400 ºC 完全消失. 当温度升到 400 ºC 时, 弱 *cis*-$(N_2O_2)^{2-}$ 吸收物种消失. 桥式硝酸盐的吸

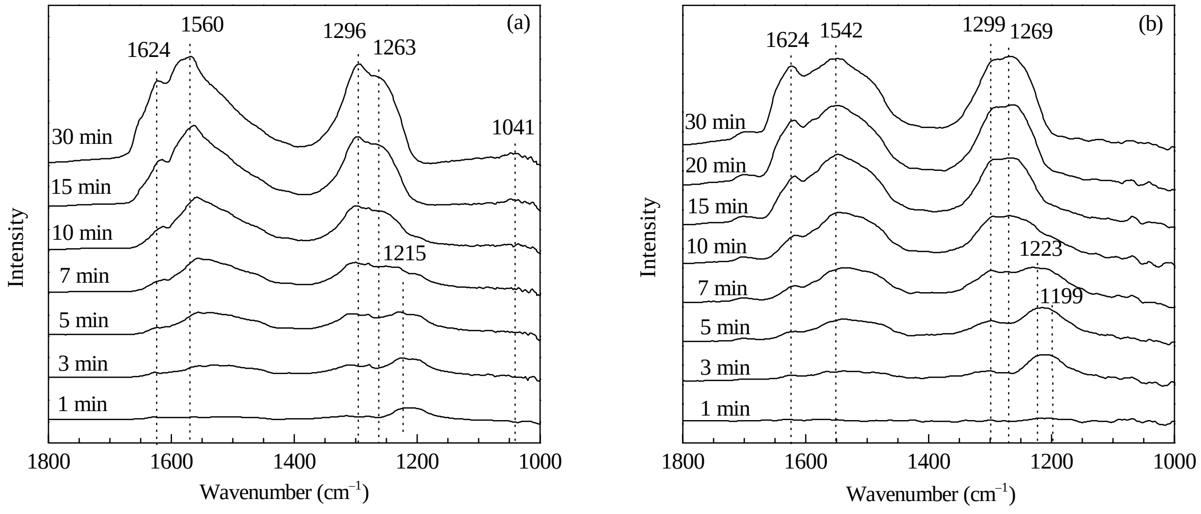

图 6　NiO/Al_2O_3-0.30(C) 和 NiO/Al_2O_3-0.30(P) 的 DRIFTS 谱

Fig. 6.　DRIFTS spectra of NiO/Al_2O_3-0.30(C) (a) and NiO/Al_2O_3-0.30(P) (b).

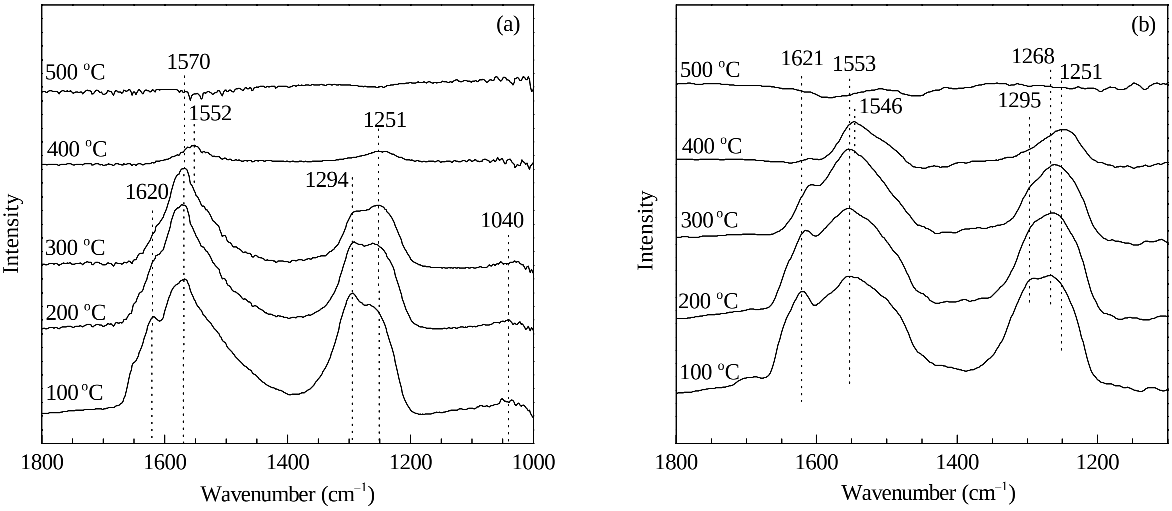

图 7 NiO/Al_2O_3-0.30(C) 和 NiO/Al_2O_3-0.30(P) 的 NO_x 脱附红外光谱

Fig. 7. DRIFTS spectra of NO_x thermal desorption of the catalyst with and without NTP treatment. (a) NiO/Al_2O_3-0.30(C); (b) NiO/Al_2O_3-0.30(P).

收峰强度在400 ℃开始减弱, 至500 ℃时完全消失.

对于 NiO/Al_2O_3-0.30(P) 样品, NO_2 物理吸附峰在300 ℃以下仍稳定存在, 至400 ℃时完全消失; 其他吸收峰在 500 ℃ 时完全消失, 这与 NiO/Al_2O_3-0.30(C) 的相同, 而且 NiO/Al_2O_3-0.30(P) 的脱附峰更宽.

比较图1和图7, 可以发现, 经NTP处理后, 催化剂上各物种吸收峰和脱附峰面积较大, 说明催化剂表面吸附物种的量增加. 然而, 目前关于低温等离子体处理催化剂的吸附机理还不十分清楚.

3 结论

NiO负载量是影响 NiO/Al_2O_3 催化剂的 NO_x 储存能力的一个因素, 当Ni:Al摩尔比为0.3时, 催化剂的 NO_x 储存量最大. NiO负载量明显影响粒子的分散性, 随着Ni含量的增加, 催化剂比表面积减小, $NiAl_2O_4$ 晶粒变小, 它对样品 NO_x 储存能力的影响较大. 经等离子体活化后, 催化剂的 NO_x 储存量增加, 当Ni:Al摩尔比为1.0时, 经等离子体处理催化剂的 NO_x 储存量是未经等离子体处理的1.46倍. 在 NO_x 的吸附过程中, NO首先以桥式亚硝酸盐形式吸附在催化剂表面, 然后变成不同形式的硝酸盐物种.

参考文献

1 Takahashi N, Shinjoh H, Iijima T, Suzuki T, Yamazaki K, Yokota K, Suzuki H, Miyoshi N, Matsumoto S I, Tanizawa T, Tanaka T, Tateishi S S, Kasahara K. *Catal Today*, 1996, **27**: 63
2 Li J H, Goh W H, Yang X C, Yang R T. *Appl Catal B*, 2009, **90**: 360
3 Wei LS, Li J H, Tang X F. *Catal Lett*, 2009, **127**: 107
4 Li J H, Li W, Yang R T. *Catal Lett*, 2009, **129**: 104
5 Cheng W H, Wu K C, Lo M Y, Lee C H. *Catal Today*, 2004, **97**: 145
6 Zhou G, Luo T, Gorte R J. *Appl Catal B*, 2006, **64**: 88
7 Xu J, Harold M P, Balakotaiah V. *Appl Catal B*, 2009, **89**: 73
8 Nova I, Lietti L, Castoldi L, Tronconi E, Forzatti P. *J Catal*, 2006, **239**: 244
9 Frola F, Prinetto F, Ghiotti G, Castoldi L, Nova I, Lietti L, Forzatti P. *Catal Today*, 2007, **126**: 81
10 Opoku-Gyamfi K, Adesina A A. *Appl Catal A*, 1999, **180**: 113
11 Seo Y S, Kang S K, Han M H, Baek Y S. *Catal Today*, 1999, **47**: 421
12 Radwan N R E, El-Shobaky G A, Fahmy Y M. *Appl Catal A*, 2004, **274**: 87
13 Lee K M, Lee W Y. *Catal Lett*, 2002, **83**: 65
14 李翠平, 赵瑞红, 郭奋, 陈建峰. 物理化学学报 (Li C P, Zhao R H, Guo F, Chen J F. *Acta Phys-Chim Sin*), 2007, **23**: 157
15 李翠平, 赵瑞红, 郭奋, 陈建峰. 北京化工大学学报 (Li C P, Zhao R H, Guo F, Chen J F. *J Beijing Univ Chem Technol*), 2007, **34**: 358
16 Wang J G, Liu C J, Zhang Y P, Yu K, Zhu X L, He F. *Catal Today*, 2004, **89**: 183
17 Cheng D G, Zhu X L, Ben Y H, He F, Cui L, Liu C J. *Catal Today*, 2006, **115**: 205
18 李秋荣, 李俊华, 贺君, 刘遥, 郝吉明. 环境化学 (Li Q R, Li J H, He J, Liu Y, Hao J M. *Environ Chem*), 2010, **29**: 721

19 Liu C J, Yu K L, Zhang Y P, Zhu X L, He F, Eliasson B. *Appl Catal B*, 2004, **47**: 95
20 Zou J J, Liu C J, Zhang Y P. *Langmuir*, 2006, **22**: 2334
21 Clayton R D, Harold M P, Balakotaiah V, Wan C Z. *Appl Catal B*, 2009, **90**: 662
22 Lenglet M, Hochu F, Dürr J, Tuilier M H. *Solid State Commun*, 1997, **104**: 793
23 Fanson P T, Horton M R, Delgass W N, Lauterbach J. *Appl Catal B*, 2003, **46**: 393
24 Su Y, Amiridis M D. *Catal Today*, 2004, **96**: 31
25 Westerberg B, Fridell E. *J Mol Catal A*, 2001, **165**: 249
26 Chen L, Li J H, Ge M F. *J Phys Chem C*, 2009, **113**: 21177
27 Chen L, Li J H, Ge M F, Zhu R H. *Catal Today*, 2010, **153**: 77
28 Li J H, Zhu R H, Cheng Y S, Lambert C K, Yang R T. *Environ Sci Technol*, 2010, **44**: 1799
29 Muncrief R L, Khanna P, Kabin K S, Harold M P. *Catal Today*, 2004, **98**: 393

英 译 文

English Text

NO_x storage-reduction (NSR) technology for lean burn exhaust treatment has been much studied in the past decade. In the conventional NSR catalysts such as $Pt/BaO/Al_2O_3$, the noble metal is the active component. The alkaline earth oxides also play a key role in NO_x storage [1–7]. NSR catalysts should have a large NO_x adsorption capacity at low temperature because of the wide temperature range it must be used in, which range from 200 to 500 ºC [8–9]. Due to the high cost of precious metals, transition metal oxides have been much investigated, especially, catalysts with NiO as the active component that have been used in many chemical reactions for their performance [10–15]. The application of a non-thermal plasma (NTP) during the preparation of a Ni-based catalyst can improve the catalyst performance [16,17]. The NO_x adsorption capability of Ni-based catalysts have not yet been reported. In this work, NiO/Al_2O_3 catalysts were prepared by coprecipitation, and the catalysts that were treated with NTP before calcination at high temperature were compared with those without a NTP treatment before calcination. The adsorption capacity of NO_x at low temperature on NiO/Al_2O_3 with a NTP treatment was investigated. A promotional mechanism was proposed on the basis of characterization results.

1 Experimental

1.1 Preparation of catalyst

The catalysts were prepared by coprecipitation. The $Al(NO_3)_3$ (200 ml 0.6 mol/L) solution and a required quantity of polyoxyethylene glycol were mixed in a 500 ml three-necked flask. Then the precipitating agent $(NH_4)_2CO_3$ was slowly added with high speed stirring at 70 ºC for 6 h. The appropriate amount of nickel nitrate solution was added to give molar ratios of Ni/Al of 0.15, 0.3, 0.45, 0.6, and 1.0 [18]. The pH of the solution was adjusted to 9 and the inorganic colloidal sol was aged at 70 ºC. After filtration and drying, the catalysts were calcined at 330 ºC for 3 h and then at 550 ºC for 2.5 h. This was for the preparation without a NTP treatment. The products were denoted as NiO/Al_2O_3-0.15(C), NiO/Al_2O_3-0.30(C), NiO/Al_2O_3-0.45(C), NiO/Al_2O_3-0.60(C), and NiO/Al_2O_3-1.0(C).

The setup for the NTP treatment has been described elsewhere [19]. When the non-thermal plasma treatment was used, the samples prepared as above were treated by NTP in air before calcination at 550 ºC with a discharge power of 80 W for 30 min. After the NTP treatment, the catalysts were calcined at 550 ºC for 2 h. These samples were denoted as NiO/Al_2O_3-0.15(P), NiO/Al_2O_3-0.30(P), NiO/Al_2O_3-0.45(P), NiO/Al_2O_3-0.60(P), and NiO/Al_2O_3-1.0(P).

1.2 Characterizations of the catalysts

The BET surface areas were measured by N_2 adsorption at –196 ºC using a NOVA4000e instrument. Prior to the measurement, the samples were degassed at 300 ºC for 2 h.

Phase identification was performed by an X-ray diffractometer (XRD, TTR-Ⅲ) operated at 60 kV voltage and 300 mA current.

H_2 temperature-programmed reduction (H_2-TPR) experiments were performed on a Micromeritics ChemiSorb 2720 using 50 mg samples. After pretreatment in N_2 at 300 ºC for 1 h, the samples were cooled down to room temperature. The reducing gas, a mixture of 10% H_2-90% Ar, at a flow rate of 50 ml/min, was used to reduce the catalysts from room temperature to 1000 ºC with a temperature ramp of 10 ºC/min.

Transmission electron microscope (TEM) images to determine the particle size were obtained using a JEOL 200CX microscope operated at 200 kV.

X-ray photoelectron spectroscopy (XPS) data were obtained with an ESCALab220i-XL electron spectrometer from VG Scientific using 300 W Mg K_α radiation. The base pressure was 3×10^{-7} Pa. The binding energies were referenced to the C 1*s* line from adventitious carbon at 284.8 eV. Binding energies (E_b) were measured for C 1*s*, O 1*s*, Ni 2*p*, and Al 2*p*. The spectra were deconvoluted using the XPSPEAK program by curve fitting with a Gaussian/Lorentian ratio of 90/10 after smoothing and subtraction of the Shirley-type background.

All spectra were measured with 4 cm^{-1} resolution between 4000–400cm^{-1} and 100 scans using a liquid nitrogen cooled

MCT detector on a Nicolet Nexus 870-FTIR.

The in situ DRIFTS measurements were carried out in a high temperature cell fitted with ZnSe windows. The samples were finely ground, placed in a ceramic crucible and manually pressed. The feed gas was flowed into the cell at a total flow rate of 100 ml/min. Prior to measurement, the samples were pretreated at 500 ºC in a mixture of N_2 and 8% O_2 for 30 min. Background spectra were collected after dwelling for 20 min at a given temperature. Sample spectra were collected after dwelling for 30 min in the mixture gas of 0.05% NO, 8% O_2, and balanced by N_2 at 100 ml/min.

1.3 NO adsorption-desorption

NO adsorption experiments were carried out in a U-shaped quartz reactor with an inner diameter of 5 mm under atmospheric pressure. The amount of catalysts was 0.5 g for each run. The samples were pretreated in 8% O_2-92% N_2 at a total flow rate of 400 ml/min at 500 ºC for 30 min, and then cooled to 100 ºC in N_2 for adsorption. When the temperature stabilized at 100 ºC, a mixture gas comprising 0.05% NO, 8% O_2, and balanced with N_2 at 400 ml/min was passed through the samples. At this stage, the concentrations of NO, NO_2, and NO_x in the outlet stream were recorded by an online Chemiluminescence NO_x analyzer (42C High Level, Thermo Electron Corporation). After adsorption for 30 min, NO and O_2 were removed and pure N_2 (400 ml/min) was introduced for 1 h to remove weakly adsorbed species on the surface of catalysts. Then temperature-programmed desorption (TPD) experiments were performed by ramping the temperature from room temperature to 500 ºC at 10 ºC /min with 400 ml/min N_2. The concentration of NO, NO_2, and NO_x in the outlet stream were also measured by the NO_x analyzer. The NO_x storage capacity (NSC) was calculated from the integral area of the desorption profile.

2 Results and Discussion

2.1 Influence of NiO loading and NTP treatment on NSC of the catalysts

The NO_x storage capacity and break through time of the catalysts with different Ni contents are listed in Table 1. No NO_x was detected in the effluent in the initial 5 min for NiO/Al_2O_3-0.15(C), NiO/Al_2O_3-0.30(C), NiO/Al_2O_3-0.45(C), and NiO/Al_2O_3-0.60(C), and in the initial 4 min for NiO/Al_2O_3-1.0(C). When the molar ratio of Ni and aluminum was 0.3, the NO_x storage capacity reached the maximum value of 345 μmol/g on NiO/Al_2O_3-0.30(C). When the NiO loading was higher or lower than that of NiO/Al_2O_3-0.30(C), the NSC of the catalyst was lower than that of NiO/Al_2O_3-0.30(C). For the catalysts that were first treated by the NTP in the preparation, the time of breakthrough clearly increased, and it was 7 min for NiO/Al_2O_3- 0.30(P), NiO/Al_2O_3-0.45(P), NiO/Al_2O_3-0.60(P), and NiO/Al_2O_3-1.0(P). The maximum NSC of 477 μmol/g was obtained on NiO/Al_2O_3-0.30(P), which was increased by 38% compared to the NSC of NiO/Al_2O_3-0.30(C). After breakthrough, the NO_x concentration in the outlet stream gradually increased to 0.07%. The results showed that it took a longer time to reach adsorption saturation on the catalysts subjected to the NTP treatment. Hereafter, the characterization was mainly with the NiO/Al_2O_3 catalyst with a Ni/Al molar ratio of 0.30 because of its higher NO_x storage capacity.

2.2 Influence of NTP treatment on NO_x desorption

It can be seen from Table 1 that the NSC of the catalysts were increased by the NTP treatment. Figure 1 shows the TPD profiles of NO+O_2 adsorption over NiO/Al_2O_3-0.30(C) and NiO/Al_2O_3-0.30(P). Three NO_x desorption peaks at 120, 200, and 430 ºC were observed on the catalysts with and without the NTP treatment.

The NSCs of NiO/Al_2O_3-0.30(P) were larger than those of NiO/Al_2O_3-0.30(C) at both low and high temperatures. NO_x desorption amounts of the catalysts with the NTP treatment were clearly enhanced in both the low and high temperature regions. The NO_x desorption peak observed at 120 ºC was related to nickel meta-aluminate ($NiAl_2O_4$). The reason is that the intensity of nickel meta-aluminate peak weakened with an increase of Ni content. The presence of nickel meta-aluminate is an important factor in NO_x storage capacity [18].

2.3 Characterization of the catalysts

2.3.1 Specific surface area

The specific surface areas are summarized in Table 2. It can be seen that the specific surface area of the catalysts decreased with increasing Ni loading. The reason is that nickel oxides supported on the carrier agglomerated so that some pores of the carrier were clogged. It is significant that the specific surface area of the catalysts with the NTP treatment increased. The probable reason is that the NTP treatment improved the dispersion of the particles.

2.3.2 XRD characterization

The XRD patterns of NiO/Al_2O_3-0.30(C) and NiO/Al_2O_3-0.30(P) are shown in Fig. 2. Two phase structures were observed: one was assigned to NiO, and the other was attributed to $NiAl_2O_4$. Fig. 2(1) and (4) show the main peaks of $NiAl_2O_4$. The peaks of $NiAl_2O_4$ in NiO/Al_2O_3 catalysts with Ni/Al molar ratio of 0.15 and 0.30 are very distinct at 19°, 31°, 37°, 45°, and 65°. The intensities of NiO/Al_2O_3 catalysts with the NTP treatment were weaker than those without the NTP treatment. The intensities of some peaks decrease as a result of the breakup of crystalline granules by the plasma treatment [20], but the peak intensity of $NiAl_2O_4$ in NiO/Al_2O_3-0.30(P) at 19° was stronger than that of NiO/Al_2O_3-0.30(C).

Figure 2(5)–(8) are the XRD patterns of NiO/Al_2O_3 catalysts with Ni/Al molar ratio of 0.6 and 1.0. However, the diffraction intensities of the catalysts with the NTP treatment were strengthened. With increasing Ni content, the intensities of the NiO diffraction peaks were enhanced. These results revealed that the catalysts had good crystalline structure. The peaks of $NiAl_2O_4$ in NiO/Al_2O_3 with Ni/Al molar ratio of 0.6 were more diffuse than those of NiO/Al_2O_3 with Ni/Al molar ratio of 0.3. The peaks of $NiAl_2O_4$ in NiO/Al_2O_3 with Ni/Al molar ratio of 1.0 had basically disappeared. The adsorption capacity of NiO/Al_2O_3 with Ni/Al molar ratio of 0.3 was the largest among the catalysts, which indicated $NiAl_2O_4$ had an obvious effect in the crystalline complex.

2.3.3 H_2-TPR characterization

H_2-TPR experiments were carried out to investigate the reducibility of the catalysts. The results are shown in Fig. 3. The NiO/Al_2O_3-0.30(C) catalyst showed one reduction peak at 318 ºC, while it was at 308 ºC for NiO/Al_2O_3-0.30(P), which was attributed to the reduction of Ni_2O_3 into NiO. The NiO/Al_2O_3-0.30(C) catalyst showed another reduction peak at 639 ºC, which was at 612 ºC for NiO/Al_2O_3-0.30(P), which can be described to the reduction of NiO into Ni.

The reduction temperature of the catalyst with the NTP treatment was lower than that of the catalyst without the NTP treatment. The peak temperature of the catalyst with the NTP treatment decreased and the peak became wider. The catalysts with the NTP treatment were easier to reduce, which would be advantageous for NO oxidation.

2.3.4 TEM characterization

TEM images of NiO/Al_2O_3 with Ni/Al molar ratio of 0.3 are shown in Fig. 4. The results showed that NiO/Al_2O_3-0.30(C) did not have good particle dispersion, and the agglomeration phenomenon of nickel oxide on the surface of catalyst was very serious. In comparison with NiO/Al_2O_3-0.30(C), agglomeration of the particles on NiO/Al_2O_3-0.30(P) was not obvious. Many particles had a highly discrete distribution in Fig. 4(b), and the particle distribution of NiO/Al_2O_3-0.30(P) was very uniform. The characteristics of the highly efficient catalysts prepared from using a NTP treatment had been studied by plasma physics and cluster physics [21], which showed that the activity of the loaded metal was greatly modified by the NTP treatment.

2.3.5 XPS characterization

The Ni $2p_{3/2}$ binding energy of the catalysts by the different treatment methods are shown in Fig. 5. The NiO/Al_2O_3-0.30(C) exhibited the Ni $2p_{3/2}$ main peak at 853.8 eV with satellites around 859.9 eV and a spin-orbit coupling energy gap of 17.8 eV. The NiO/Al_2O_3-0.30(P) exhibited the Ni $2p_{3/2}$ main peak at 854.4 eV with satellites around 860 eV and a spin-orbit coupling energy gap of 16.9 eV. The Ni $2p_{3/2}$ E_B of pure NiO is 854.5 eV while for $NiAl_2O_4$ spinel, it appears at 856 eV. The Ni $2p_{3/2}$ E_B of NiO/Al_2O_3-0.30(P) was slightly higher than that of NiO/Al_2O_3-0.30(C), which reflected the different surface elements present [22]. Table 3 shows the relative amounts of surface nickel and oxygen. The amounts of nickel and oxygen on the surface of the catalyst increased after the NTP treatment. The amount of $NiAl_2O_4$ on the surface of the catalyst treated by NTP was more than that of the catalyst without the NTP treatment, so the Ni $2p_{3/2}$ E_B of NiO/Al_2O_3-0.30(P) was higher than that of NiO/Al_2O_3-0.30(C). This was consistent with the NO_x-TPD results.

2.4 FT-IR spectra

2.4.1 NO_x adsorption

In situ DRIFTS of NiO/Al_2O_3-0.30(C) and NiO/Al_2O_3-0.30(P) during adsorption of 0.05% NO in the presence of 8% O_2 at 100 ºC are shown in Fig. 6. The adsorption peaks of the species on the surface of the catalysts were between 1000–1800 cm^{-1}. The peak at 1040 cm^{-1} can be assigned to *cis*-$(N_2O_2)^{2-}$, that at 1205 cm^{-1} nearby can be assigned to bridging nitrite, and those at 1260, 1400, and 1560 cm^{-1} were assigned to different nitrates. The peak at 1620 cm^{-1} nearby can be assigned to physical adsorbed NO_2 [23,24].

When adsorption began on the surface of the catalysts, there were mainly bridging nitrite (1215 cm^{-1}) and weakly adsorbed NO_2 species (1624 cm^{-1}) [25]. After 3 min, the adsorption peak at 1624 cm^{-1} became obvious and bridging nitrate (1560 cm^{-1}) species appeared. After 5 min, the adsorbing peak of nitrate adsorbed species became obvious. After 7 min, the adsorption species changed into bridging nitrite (1263 cm^{-1}), monodentate nitrate (1296 cm^{-1}), bridging nitrate (1560 cm^{-1}), and NO_2 adsorbed species(1624 cm^{-1}). After 10 min, the adsorbed species intensity of *cis*-$(N_2O_2)^{2-}$ (1040 cm^{-1}) increased, and simultaneously, bridging nitrite (1263 cm^{-1}), monodentate nitrate (1296 cm^{-1}) , bridging nitrate(1560 cm^{-1}), and NO_2 adsorbed species (1624 cm^{-1}) existed on the surface of catalysts. The adsorption peaks at 15 and 30 min were the same as those at 10 min [26–29]. The DRIFTS spectrum of NiO/Al_2O_3-0.30(P) is shown in Fig. 6(b). When adsorption began on surface of the catalyst, there was mainly bridging nitrite (1199–1223 cm^{-1}). After 10 min, the adsorbed species were mainly bridging nitrite (1269 cm^{-1}), monodentate nitrate (1299 cm^{-1}), bridging nitrate (1542 cm^{-1}), and a small amount of NO_2 physically adsorbed (1624 cm^{-1}). There were no adsorbed species of *cis*-$(N_2O_2)^{2-}$ (1040 cm^{-1}) on the catalyst surface. The adsorption peak bands of NiO/Al_2O_3-0.30(P) were broader than those of NiO/Al_2O_3-0.30(C).

2.4.2 Thermal desorption of NO_x species

Further information on the nature of the surface species observed in the NO/O_2 adsorption experiments were gained from thermal desorption studies. Figure 7 shows the results of NO_x desorption from NiO/Al_2O_3-0.30(C) and NiO/Al_2O_3-0.30(P). In Fig. 7(a), it can be seen that the physically adsorbed NO_2 with its characteristic band at 1620 cm^{-1} was stable to 200 ºC. The bands at 1294 and 1251 cm^{-1} decreased gradually and vanished at 400 ºC. As the temperature increased to 400 ºC, the weakly adsorbed species at 1040 cm^{-1} vanished. The intensity of bridging nitrate (1570 cm^{-1}) bands started to decrease at 400 ºC and had completely disappeared by 500 ºC. In Fig. 7(b), physically adsorbed NO_2 with its characteristic band at 1621 cm^{-1} was stable to 300 ºC and it disappeared at 400 ºC. The other peaks of NiO/Al_2O_3-0.30(P) had completely vanished at 500 ºC , which was the same result as that of NiO/Al_2O_3-0.30(C). The desorption peak bands of NiO/Al_2O_3-0.30(P) also became broad.

On comparing the desorption temperature in the NO_x-TPD spectra (Fig. 1) and the DRIFTS spectra of the thermal desorption experiment (Fig. 7), the NO_x-TPD spectra indicated that the areas of the adsorption peaks and desorption peaks on catalysts with the NTP treatment became larger. This indicated that the amounts of adsorbed species on the catalysts with the NTP treatment were larger than that on the catalysts without the NTP treatment. However, the adsorption mechanism on the catalysts with the NTP treatment is not yet known.

3 Conclusions

NiO loading was one factor that influenced the NO_x storage capacity of NiO/Al_2O_3 catalysts. The optimum NiO loading was 30% molar ratio. The NiO loading affected the dispersion, and with increased Ni loading, the specific surface area of the catalyst decreased. The nickel meta-aluminate diffraction peaks weakened with increased Ni loading, and nickel meta-aluminate could be a key phase for NO_x storage capacity. The storage capacities of NO_x on the catalysts prepared with a NTP were higher than those on the catalysts without the NTP treatment. The NO_x storage capacity of NiO/Al_2O_3 with the NTP treatment was 1.46 times larger than that of NiO/Al_2O_3 (molar ratio of 1 for Ni and Al) without the NTP treatment. The DRIFTS results indicated that during NO_x adsorption on the catalysts, NO was first adsorbed on the surface as bridging nitrites, and then the nitrite species transformed into different kinds of NO_3^- adsorbed species.

Full-text paper available online at ScienceDirect
http://www.sciencedirect.com/science/journal/18722067